36th AIAA Fluid Dynamics Conference and Exhibit
5 - 8 June 2006, San Francisco, California

AIAA 2006-3367

An Experimental Study of the Far-Field of Incompressible Swirling Jets

Abolfazl F. Shiri* and William K. George†

Chalmers University of Technology, Götebory, SE-41296, Sweden

Jonathan W. Naughton‡

University of Wyoming, Laramie, WY, 82071, USA

The far field of an incompressible swirling jet has been studied using two-dimensional laser Doppler anemometry. Three pairs of symmetric injectors were used to produce weak-to-moderate swirling jets. Velocity profiles of the mean and fluctuating stream-wise and azimuthal velocity components were measured in jets with two levels of swirl ($S = 0.15$ and 0.25) at axial locations up to 50 jet exit diameters. The velocity and turbulence intensity profiles, centerline decay, and growth rates for the various swirling jets are compared to those obtained in the same facility without swirl ($S = 0$). Like the previous observations for the near jet,[1,2] there was no observable effect on the properly scaled far jet for the $S = 0.15$ case. The results were virtually identical to the non-swirling jet. For the $S = 0.25$ case, the only statistically significant effect was a shift in the virtual origin (from $x/D_* = 0.75$ to -2.9). The recent predictions of equilibrium similarity theory[3] were found to be in excellent agreement with the experimental results. In particular, the mean azimuthal component of velocity falls off as the inverse square of the downstream distance. By contrast, the mean stream-wise velocity and turbulence intensities fall off with the inverse of the downstream distance. As a consequence, the mean azimuthal equation uncouples from the rest, so the asymptotic swirling jet behaves like the non-swirling jet.

Nomenclature

A, B_u, C	growth rate constants for self-preserving axisymmetric jet
D	nozzle exit diameter
G	degree of swirl $\equiv \frac{W_{max0}}{U_{max0}}$
G_θ	axial component of angular momentum flux
$\mathcal{T}_{int}$	integral time scale
L	axial length scale
M_x	axial momentum flux
N_{eff}	number of effectively independent samples
Re_D	Reynolds number based on the jet diameter
R	nozzle exit radius
S	swirl number $\frac{G_\theta}{M_x R}$
T	total measurement time
U, V, W	mean axial, radial and tangential velocity components in the flow, respectively
U_0	average exit axial velocity
f	normalized axial velocity function in the momentum integral
g	normalized azimuthal velocity function in the momentum integral
m_x	mass flux in axial direction
u, v, w	fluctuating axial radial and azimuthal velocity component, respectively

*Ph.D. Student, Department of Applied Mechanics, Chalmers University of Technology, AIAA Member.
†Professor, Department of Applied Mechanics, Chalmers University of Technology, AIAA Associate Fellow.
‡Associate Professor, Mechanical Engineering Department, Dept 3295, AIAA Associate Fellow.

x, r, θ	cylindrical coordinate system
x_o	virtual origin for self-preserving axisymmetric jet
α	thermal diffusivity
β	volumetric thermal expansion coefficient
$\delta_{1/2}$	jet half-width
$\epsilon^2_{\psi_N}$	relative statistical error of estimator ψ_N
ε_ν	viscous dissipation
η	normalized radial coordinate in the momentum integral

Subscripts

c	center line
max	maximum value
o	jet, nozzle exit condition
∞	free stream or ambient conditions
$*$	scaled property

I. Introduction

TURBULENT jets have continued to interest researchers for many years, both because of their numerous applications as well as their importance to our fundamental understanding of turbulence. Jet flows with swirl are of particular interest, especially in combustion, and many experimental and theoretical studies have tried to address the questions of the stability and dependency on initial condition of jet flow. But even the non-swirling axisymmetric jet has proven a considerable challenge to researchers, and only recently has the role of upstream conditions and downstream similarity been fully recognized.[4–6] Only with this recognition has it become possible to sort out the apparently conflicting results for even the single point turbulence statistics.[7,8]

Swirling jets add to the interest of this class of flows because swirl can be considered as a significant change in the jet flow's initial conditions. Farokhi et al. [9] and Gilchrist and Naughton[2] investigated the effect of swirl on the near-field flow of an axisymmetric jet and showed that moderate swirl (below vortex breakdown) enhances the growth rate and mixing compared to those of a non-swirling jet. The latter presented evidence that the enhanced growth rates persisted to 20 diameters downstream of the jet exit, even though the swirl had decayed to a point where it was barely detectable.[2] Such changes in the flow characteristics in the near-field would suggest that some turbulence structure of the swirling jet must persist far downstream.

Although swirling jets have been studied for a long time, detailed measurements of the far-field flow under carefully controlled conditions are lacking. The objective of the present study is to make such measurements in the jet far field using laser Doppler anemometry (LDA) to complement our existing knowledge of these flows. The LDA data acquired here are used to assess the characteristics of the swirling jet in the far-field and compare these results with those in the near field. By contrast with the earlier studies of the near field, the present results for the far jet show a linear growth rate for the far field of swirling jet that is the same as for the non-swirling jet. Moreover, *if the statistical moments are properly scaled using the rates at which momentum and mass are added at the source*, there appears to be no effect of swirl in the far-field other than to move the virtual origin of the flow. The overall findings substantiate theDetails of the early development of a real jet. theoretical analysis of Ewing[3] who used equilibrium similarity considerations to argue that the effects of swirl on the asymptotic jet should be negligible.

In the following sections, the implications of the governing equations and the similarity results are reviewed. It is argued that the swirl introduces another length scale into the problem, with consequence that the swirl number is a ratio of length scales. Next the experimental facility and experiments are described and the data presented. Finally the implications of the similarity analysis on the results are considered.

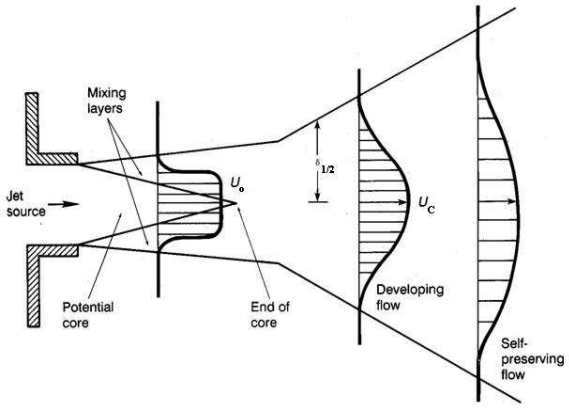

Figure 1. Schematic of the early development of a jet.

II. Implications of the Governing Equations

A. Basic scaling parameters

The basic equations have been carefully reconsidered recently by Ewing[3] and Shiri.[10] Of primary concern for this paper are the two fundamental integrals of the RANS equations for the fully developed asymptotic turbulent swirling jet. The the first is M_x, which is the total rate of transfer of kinematic linear momentum across any downstream plane, say at location x. At high Reynolds numbers and in the absence of an external flow this reduces to:

$$M_x = 2\pi \int_0^\infty \left[U^2 - \frac{W^2}{2} + \langle u^2 \rangle - \frac{\langle v^2 \rangle + \langle w^2 \rangle}{2} \right] r dr \tag{1}$$

Moreover, since there are no forces acting on any control volume containing this plane and the exit plane of the jet, M_x must remain equal to its source value, M_o, at all downstream positions, x.

The second fundamental parameter, G_θ, is rate which kinematic angular momentum is swept across any downstream plane. From integration of the angular momentum equation with the same assumptions as above this reduces to:

$$G_\theta = 2\pi \int_0^\infty [UW + \langle uw \rangle] r^2 dr \tag{2}$$

Like the linear momentum, G_θ, should remain constant at its source value, G_o, since in an infinite environment there are no torques acting on any control volume containing the source plane and any plane that cuts perpendicularly through the jet axis.

B. The effect of mass addition at the source

A third integral provides the rate at which volume (kinematic mass) is swept across any downstream plane:

$$m_x = 2\pi \int_0^\infty U r dr \tag{3}$$

Unlike M_x and G_θ, m_x is not constant at the rate at which kinematic mass is being added at the source, m_o, since mass is being continually entrained by the jet. Nonetheless, in non-swirling jets, m_o (together with M_o) sets the virtual origin of the jet, since it imposes a length scale, D_*, at the exit plane. D_* is the effective diameter defined by:

$$D_* = \sqrt{\frac{m_o^2}{M_o}} \tag{4}$$

In fact it is the ratio of the axial distance, x to this length scale that measures the evolution of the near jet into the far jet. In particular, it is only when $x >> D_*$ that the asymptotic free jet can be reached. Or said another way: only when the mass entrained by the turbulence overwhelms that added at the source close the jet.

Addition of mass at the source also introduces a velocity scale, U_*, into the problem. U_* is defined by:

$$U_* = \frac{M_0}{m_0} \tag{5}$$

Both D_* and U_* can be replaced by simply the exit diameter, D and exit velocity, U_o, **if (and only if)** the exit profile has top-head form (i.e., uniform velocity across the exit plane). This is easy to see since in the top-head case:

$$D_* = \frac{\sqrt{\pi}}{2} D \tag{6}$$

$$U_* = U_0 \tag{7}$$

Much confusion in the history of the study of turbulent jets has resulted from the failure to recognize the importance of using D_* and U_* if the exit profile is not a top-hat. And often alleged effects of source conditions can eliminated with proper scaling. As will be shown below, proper scaling becomes even more important when swirl is introduced, since the effect of G_o is to introduce yet another length scale into the problem.

C. The role of swirl

It is easy to show that addition of both linear and angular momentum imposes another length scale, L_*, onto the flow, even without mass addition at the source (i.e., point sources of linear and angular momentum). L_* can be defined as:

$$L_* = \frac{G_o}{M_o} \tag{8}$$

It is immediately obvious that if mass is also added, then another length scale ratio, the so-called swirl number, can be defined:

$$S_* = \frac{G_o}{M_o D_*} \sqrt{\pi} \tag{9}$$

Note that the factor of $\sqrt{\pi}$ has been inserted into equation 9 to make it reduce to the usual definition for top-hat exit profiles (which seldom can be achieved when swirl is present); i.e.,

$$S = \frac{2G_o}{M_o D} \tag{10}$$

Clearly we should expect L_* to replace D_* as the length scale governing downstream behavior only when the swirl number is large (in much the same manner that x replaces D_* for the far non-swirling jet). Since (as will be reviewed below) the effect of angular momentum on the flow diminishes as the flow evolves downstream, at low swirl numbers, L_* will provide an indication of a measure of at most a change in the virtual origin of the asymptotic swirling jet.

D. Equilibrium similarity implications for the far swirling jet

The similarity of the asymptotic swirling axisymmetric jet has recently been reconsidered.[3,10] The results can be summarized as follows.

- The profiles of mean streamwise velocity and turbulence normal stresses can be described by single length and velocity scales. The convenient choices (and those used to scale the data in this paper) are U_c, the centerline velocity, and $\delta_{1/2}$, the velocity half-width (defined as the distance from the centerline at which the mean velocity falls to half its centerline value). Thus the normalized radial coordinate is $\eta = r/\delta_{1/2}$, exactly like the non-swirling jet.

- The spreading rate of the asymptotic jet is linear; i.e.,

$$\delta_{1/2} = A(x - x_o), \tag{11}$$

  where x_o is a virtual origin which can depend on the Reynolds number and swirl number. The coefficient A (or $d\delta_{1/2}/dx$) can in principle at least depend on the jet exit conditions. Both sides can be normalized by D_*, but normalization by D introduces a dependence on the exit profile (which can be non-uniform with swirl). Note that the result of equation 11 is not particularly straightforward to obtain (unless the analysis is done incorrectly), but follows from a detailed consideration of the Reynolds shear stress equations and the behavior of the dissipation.[4,8]

- The Reynolds shear stress scales,$< uw >$ with $U_c^2 d\delta_{1/2}/dx$. The linear growth of the far jet implied by equation 11 means that the factor of $d\delta_{1/2}/dx$ is constant, so these moments scale the same as the turbulence intensities. However, it should be noted that the dependence of the coefficient on upstream conditions means that scaled profiles may differ from experiment to experiment.

- From the conservation of linear momentum, equation 1, it follows immediately that the mean centerline velocity falls asymptotically inversely with increasing $\delta_{1/2}$. Although this is well-known[4,8] it is instructive to review briefly the reasons since similar considerations apply to the angular momentum considered below. First ignore for the moment the swirl and turbulence contributions and substitute the similarity profile for the mean velocity into equation 1 to obtain:

$$M_x = [U_c^2 \delta_{1/2}^2]\ 2\pi \int_0^\infty f^2\ \eta d\eta \tag{12}$$

  Since the integrand depends only on the similarity variable η that is integrated over the entire domain, all of the x-dependence on the right-hand side is in the square-bracketed term. But the left-hand side is equal to a constant since $M_x = M_o$. Therefore, U_c must be inversely proportional to $\delta_{1/2}$; i.e.,

$$U_c \propto \delta_{1/2}. \tag{13}$$

  Inclusion of the turbulence terms only modifies the constant of proportionality, since they too can be shown to scale with U_c^2. The swirl contribution (from the radial pressure gradient), $W^2/2$ will be shown below to vanish downstream relative to the other terms, so the effect of its omission decreases with distance.

  Combining equation 13 with the linear growth rate of equation 11 implies that:

$$U_c = B_u \frac{{M_o}^{1/2}}{(x - x_o)} \tag{14}$$

  where B is a constant and x_o must be the same virtual origin as in equation 11 above. In fact B and A can not be independent, but must also be linked to each other and the shape of the profile through equation 1. Alternatively the centerline velocity can be normalized by U_*:

$$\frac{U_*}{U_c} = \frac{1}{B_u}\left[\frac{x}{D_*} - \frac{x_0}{D_*}\right]. \tag{15}$$

  Note that U_o can be also used if the exit profile is top-hat, but if it is not, then this introduces an artificial dependence on jet exit conditions.

- The mean azimuthal (or swirl) velocity component scales with its maximum value at any cross-section, W_{max}, **and falls off as the inverse square of $\delta_{1/2}$ (or $x - x_o$).** This is a surprising result (originally proven by Ewing[3]), but can be seen immediately by substituting similarity profiles for the mean velocity, say $U/U_c = f(\eta)$, $W/W_{max} = g(\eta)$, into the angular momentum integral of equation 2. Since $\langle uw \rangle = 0$, the result is:

$$G_x = [U_c W_{max} \delta_{1/2}^3] \; 2\pi \int_0^\infty f \; g \; \eta^2 d\eta \tag{16}$$

The integral in similarity variables can at most depend on the exit conditions and is independent of x. Also the left-hand side is constant since conservation of angular momentum requires that $G_x = G_o$. Using equation14 implies:

$$W_{max} \propto [U_c \delta_{1/2}^3]^{-1} \propto [\delta_{1/2}]^{-2} \tag{17}$$

It follows immediately from equation 11 that the swirl velocity, W_{max} falls off inversely with the square of the downstream distance. In fact,

$$W_{max} = C \frac{G_o}{{M_o}^{1/2}(x - x_o)^2} \tag{18}$$

where C is a constant (at most dependent on the jet exit conditions) and x_o must be the same virtual origin as for all the other quantities. Note that, just as A and B are linked by the linear momentum integral, C is linked to both by the angular momentum integral.

Since the mean velocity falls off only inversely with distance, but the swirl falls off as inversely with the square of distance, the swirl should appear to die off. This is exactly what was noted in the experiments of Gilchrist and Naughton,[2] the swirl dies off downstream. Moreover, as first pointed out by Ewing,[3] this means the asymptotic swirling jet should behave exactly as a non-swirling jet, with at most different values of A, B and C which could in turn depend only on the jet exit conditions. A particular goal of the experiments described below was to test if and how these things happen.

Note the fact that the swirl appears to die out relative to the stream-wise flow does not mean it is gone: angular momentum is still being conserved, it's just being spread over a larger area. The spreading rate of the azimuthal velocity component is much faster than the spreading rate of the axial velocity. This can be examined from near-field measurements. As a consequence the swirl (or azimuthal mean equation) uncouples itself and plays no role in the evolution of the stream-wise and radial equations which behave as though the jet were non-swirling.

III. Experimental Setup

A. Jet Facility

The free jet used in the experiment is shown in Figure 2. It was an existing Turbulence Research Laboratory facility[8]) that was modified to produce both axial and tangential velocity at the exit. Two contractions were used to reach the jet exit diameter of 25.4 mm (one inch). One blower was used to supply axial flow, and six 15 mm injectors connected to a different blower were used to add the swirling component independently. The resulting swirling jets had a solid-body like swirl distribution at the nozzle exit. As noted by Hussein et al.[8] (see especially the appendix), there can be significant differences between a jet in a confined or semi-confined enclosure and one in an infinite environment because of the re-circulating flow entrained by the jet. The $10m \times 3.5m \times 3.5m$ enclosure was designed to minimize the back-flow momentum to at least 100 diameters, and also to provide uniform spatial seeding for the LDA measurement. A closed loop circulation was achieved by placing the blower inlet inside the tent, but far from the jet exit.

B. Laser Doppler Anemometry Method

A two-component Laser Doppler Anemometry system (Dantec) was used in a backscatter arrangement for the present study. The flow was seeded with an aerosol and bursts produced by particles passing through the control volume were analyzed by Dantec BSA burst processors. The sampling rate of the LDA system was

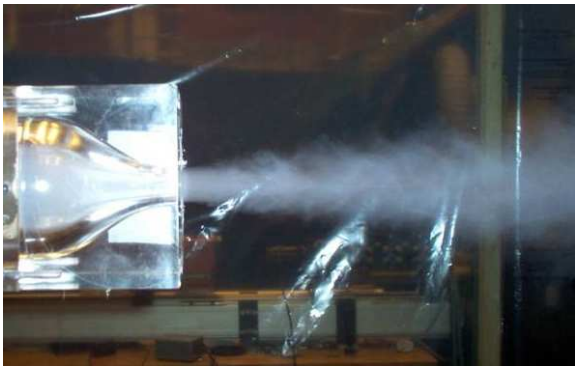

Figure 2. Photograph of jet nozzle and exit flow using smoke for visualization.

not fixed, but rather a "burst" mode was used where all particles were sampled as they arrived. The particles produced by SAFEX fog generator which generates a dense white fog by evaporation and condensation of a water-based fog liquid. The mean droplet size was around $1\mu m$ and the a closed loop of air circulation kept the particle density constant during the measurement. Selecting a seeding particle is the compromise between signal amplitude and the particles ability to follow the flow. Larger particles will increase signal quality, data rate or reduce demand for illumination, but will have a slip in accelerating flows, e.g. a high frequency turbulence. Smaller particles will reduce signal amplitude and data rate or increase demand for illumination, but will follow the flow to higher frequencies. The selected particle has the ability to follow the air flow fluctuations up to 10kHz

The particle time constant was estimated to be approximately 2.3 μs which can be compared to the smallest Kolmogorov microtime (at $x/D = 10$) which was estimated using the results of Hussein et al.[8] as 160 μs.

C. Statistical Uncertainty

All statistical moments were computed using the residence time weighting[11,12] as employed by Hussein et al.[8] A fixed sampling period of 200 seconds was used, and, in most locations, the number of samples was at least 40,000 at each point in high velocity regions and more than 4,000 at regions with velocity less than one meter per second. The largest estimate of the integral time was 0.25 s., so the minimum number of effectively independent samples was 400. Thus the relative statistical error estimate can be estimated as:[13]

$$\epsilon^2_{\psi_N} = \frac{1}{N_{eff}} \frac{var(\psi_N - \langle\psi\rangle^2)}{\langle\psi\rangle^2} \tag{19}$$

where ψ is the statistical quantity being estimated and ψ_N is is estimator using N independent estimates. The relative statistical error for the mean streamwise velocity, U, is estimated to be less than 2.5 %, and at most 7 % for the second moment statistics.[13]

Most problematical for these measurements was the mean swirl velocity, W, for which equation 19 reduces to:

$$\epsilon^2_{W_N} = \frac{1}{N_{eff}} \frac{\langle w^2\rangle}{W^2} \tag{20}$$

The mean square azimuthal velocity, $\langle w^2\rangle$, is about equal to the other turbulence normal stresses (and scales with U_c^2, but the expected value of W drops rapidly with increasing x (as noted above). Therefore, even if great care is taken in aligning the optical system to enable accurate measurement of W, statistical errors greatly complicate its determination. At the farthest downstream location, the relative statistical error of the measurement of W_{max} was estimated to be 23 %. Note that similar problems occur for the measurement of the radial component, but these can be overcome by computing V from U using the continuity equation (at least if similarity is established).

D. Test Cases

Surveys were made a several locations downstream ($x/D = 5, 10, 20, 25, 30, 35, 40, 50$) and also at the jet exit. The latter measurements were necessary to quantify the rates at which mass, momentum and angular momentum were added to the flow. These were crucial in scaling the data, and in establishing the swirl number of each for the flow. As will be illustrated below, the exit axial velocity profiles for the two flows differed slightly from the near top-hat of the non-swirling jet. As a consequence, a simple scaling with the source velocity was neither possible nor desirable.

Mean velocities in the axial and azimuthal direction at the exit of jet have been measured in order to calculate the swirl strength and Reynolds number of the jet flow. A list of the test cases is provided in Table 1, where each case has been listed by its swirl strength, S. The axial and tangential velocities have been adjusted in order to produce three cases of flow in the same Reynolds number range $Re = 45,000$.

Table 1. Test cases for the present study.

Case Number	Sn	$U_{c,0}$, m/s	$W_{max,0}$, m/s	U_*, m/s	D_*, mm	M_o	m_o	S_*
Case1	0	26.3	0	25.9	22.7	0.347	0.0268	0
Case2	0.15	27	6.7	24.8	22.9	0.323	0.0260	0.145
Case3	0.25	28.4	10	22.9	23.5	0.289	0.0252	0.239

IV. Results

A. Exit Velocity Profiles

The exit velocity profiles for the three cases are shown in figure figure 3. The non-swirling jet has a top-hat axial mean velocity profile at the jet exit. But the swirling jet profiles all exhibit profiles with a peak axial velocity on the centreline. Also the magnitude of the centreline velocity increases with increasing swirl number. Similar axial profiles have been observed by Gilchrist an Naughton[2] and Farokhi et al.[9] Panda and McLaughlin[14] also saw this peak and provided an explanation based on vortex tubes becoming spirals.

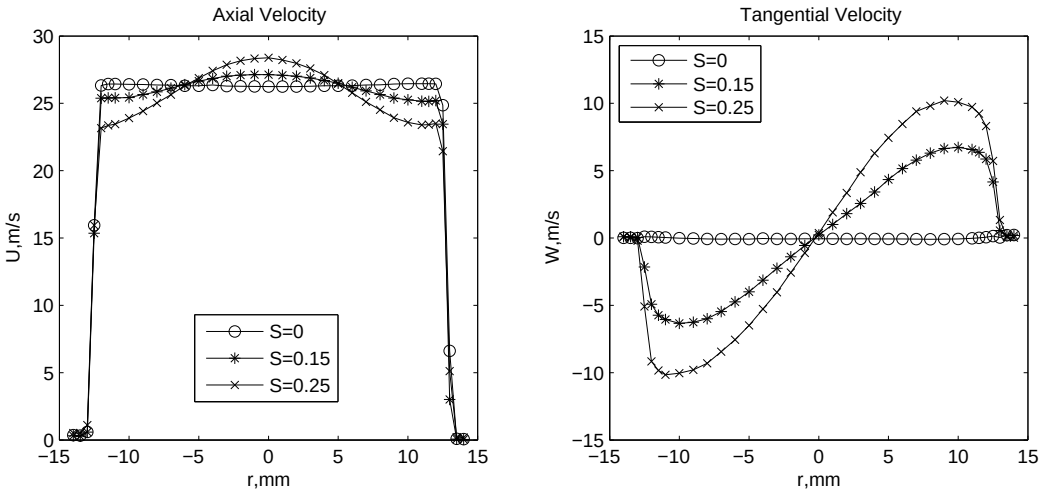

Figure 3. Axial and tangential velocity profiles at the jet exit in three different swirl number.

B. The mean velocity profiles in the far jet

It is clear from Figure 3 that the velocity profiles for the swirling jets are not a top-hat profiles, nor is the centerline velocity at the exit representative of the exit flow. Therefore, in order to have a reliable

comparison between three different cases, it is necessary to scale the far jet data with the D_* and $U_{\circ *}$ (defined by equations 4and 5 respectively). Figure 4 shows the normalized mean axial velocity profiles for all three cases ($S = 0$, 0.15, and 0.25) and all downstream positions ($x/D_* = 20, 25, 30, 35, 40$ *and* 50). The radial direction has been normalized by $\delta_{1/2}$, the jet half-width (determined as described in the next section). In all three cases, the normalized velocities show collapse of the data for all cross sections in the far-field region of the jet. Moreover, there is very little (if any) difference from one set of data to the next. Both of these observations are consistent with the theory presented earlier that the far asymptotic swirling jet should appear to be independent of swirl.

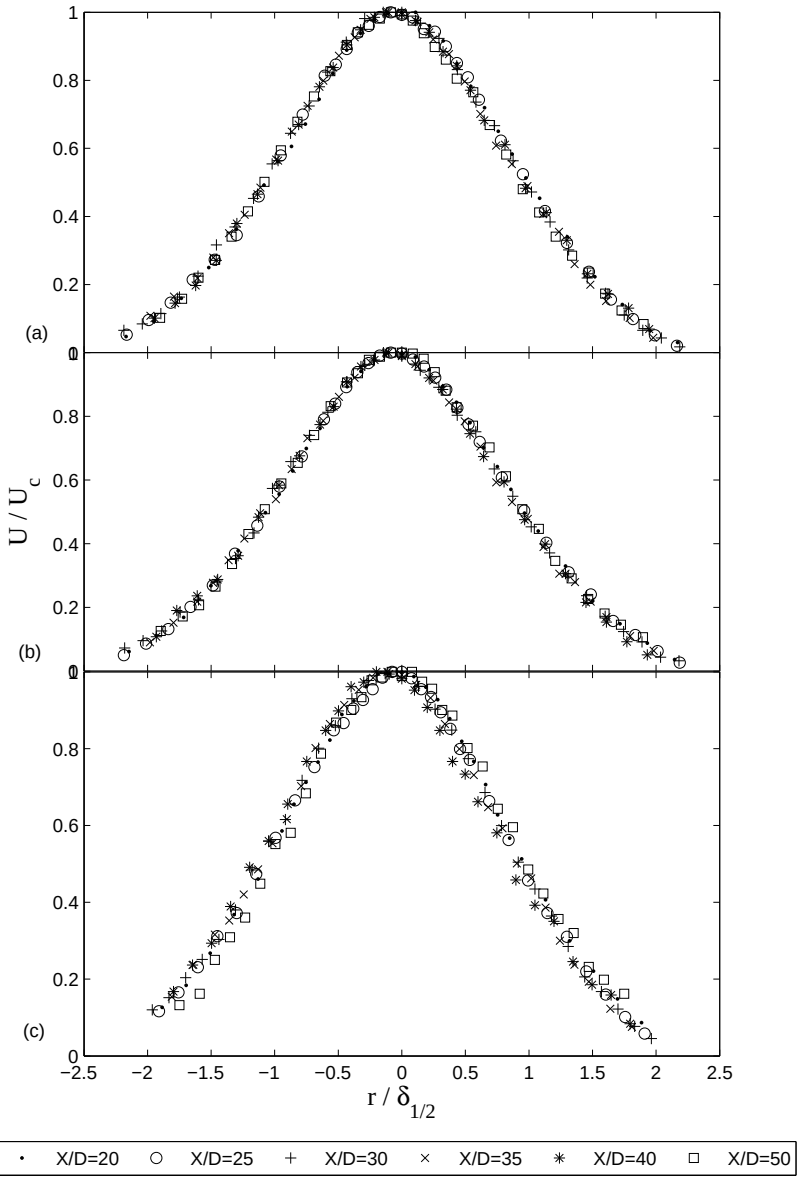

Figure 4. Mean stream-wise velocity at different axial position for the three different cases: (a)S=0, (b)S=0.15, (c)S=0.25. The profiles have been normalized by the local mean centerline velocity, U_c, the half-width, $\delta_{1/2}$.

C. Variation of U_c and $\delta_{1/2}$ with x

The jet velocity half-width is defined as the distance between the centerline and the location where the axial velocity drops to half of the centerline velocity. In order to calculate these values for each curve, the following empirical jet profile was fitted to each profile:[2]

$$\frac{U}{U_c} = sech^2\left(a\frac{r}{x}\right). \tag{21}$$

The results are shown in Figure 5. The solid lines drawn on the figure for $S = 0$ and $S = 0.15$ are

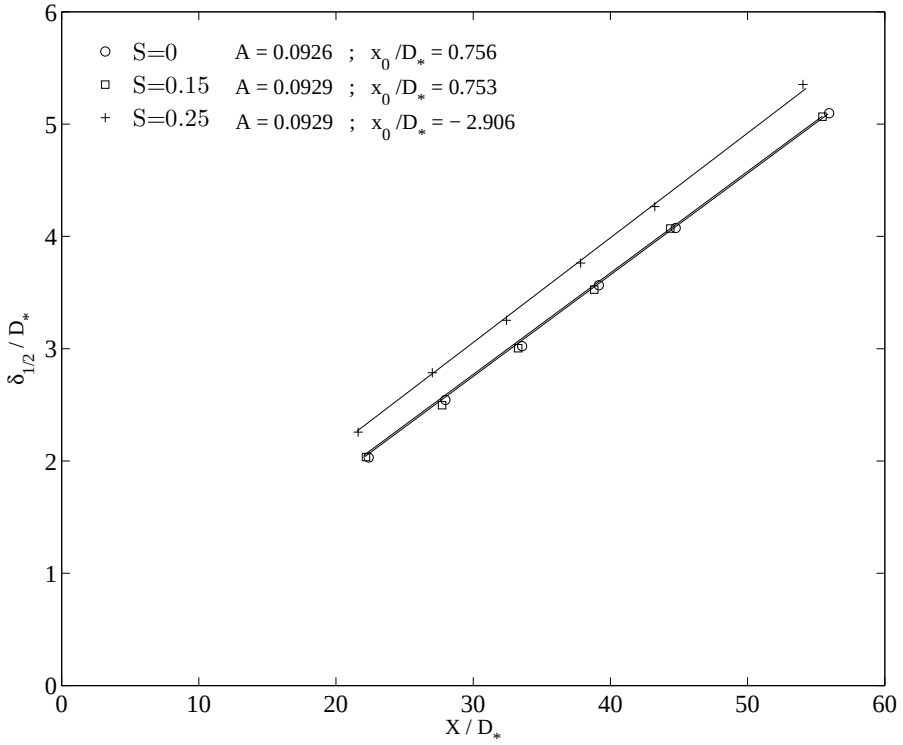

Figure 5. Streamwise variation of the velocity profile half-width plotted as $\delta_{1/2}/D_*$ versus x/D_*.

regression fits of equation 11 with both sides divided by D_*. For both, the slope of the curves, A, is 0.093 and the virtual origin is at $x_o = 0.75$. The value of A is very close to the value of $A = 0.94$ in the non-swirling jet of Hussein et al. [8] The virtual origin, however, is closer to the exit plane, undoubtedly reflecting the differences in the way the flows were generated.

The same regression fit to the $S = 0.25$ case yields 0.96 and -3.2 respectively. Drawn instead on the $S = 0.25$ data is a solid line with the same slope as for the $S = 0$ and 0.15 cases, which clearly provides an almost equally good fit to the data. This suggests strongly that there is really no statistically significant difference the the spreading rate for the three swirl values. There is most certainly, however, a change in virtual origin, which even with the modified curve fit has moved from the zero and low swirl values to $x_o = -2.9$. The fact that there are no differences at all when $S < 0.2$ is consistent with the earlier observations that the swirl number must exceed this value for any effect to be noticed on the near field.[1,2]

The mean stream-wise centreline velocity is plotted as a function of downstream location in Figure 6 in the region where the jet can be assumed to be self-preserving ($x/D_* > 20$). The solid line curves shown are regression fits of equation 15. Since the local centreline velocity appears in the denominator of the ordinate, the $1/(x - x_o)$ decay rate is manifested as a straight line in the figure, the slope of which is $1/B_u$. For the $S = 0$ and $S = 0.15$ jets, the values of B_u are nearly identical at 6.87 and 6.86 respectively, and the virtual

origins are the same at $x_o = 0.75$. (Note that the virtual origins are the same as for the curve fits to $\delta_{1/2}$, *as they must be.*). These values are slightly higher than then equivalent value from Hussein et al.,[8] which when converted from D_* to D yield $B_u = 6.55$, perhaps reflecting the residual role of W^2 in equation 1.

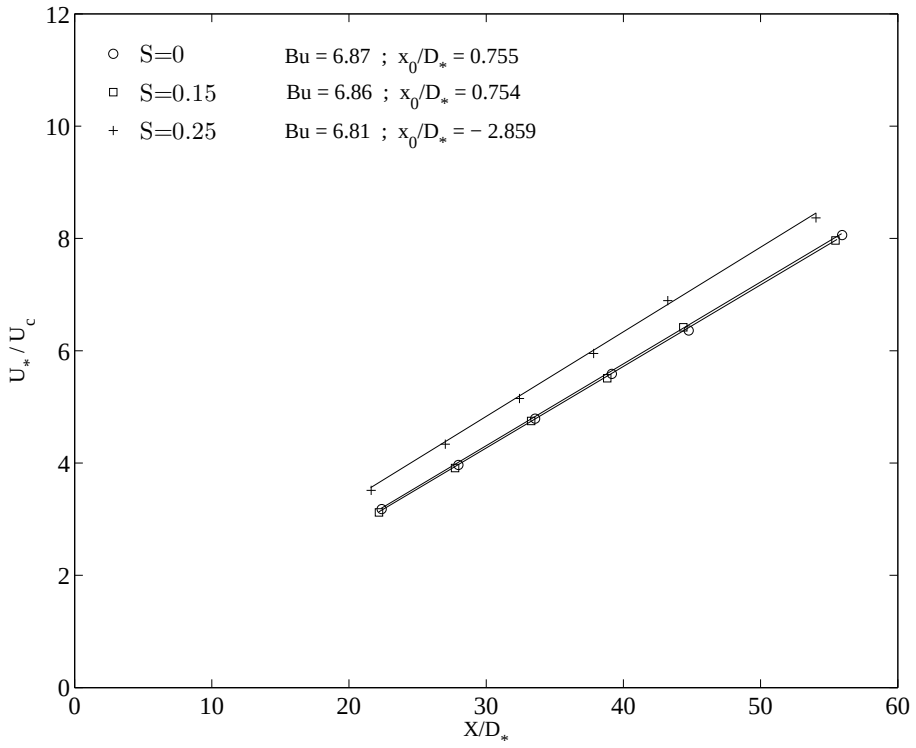

Figure 6. Streamwise variation of centerline mean velocity plotted as U_*/U_c versus x/D_*.

The regression fit to the data for the $S = 0.25$ case yields a somewhat smaller value of $B_u = 6.61$ case with a virtual origin of -1.65. But as with the half-width plots above, a curve can be drawn on this data with the same slope as the others; only the virtual origin need be modified.

Therefore the data as plotted behave according to the expected linear functions of the axial distance. To within the statistical error it seems that there is no change on either the spreading rate or the rate at which the centerline velocity decays, other than the change in virtual origin for the $S = 0.25$ case. The fact that this shift occurs for $S > 0.2$ is consistent with the changes observed by others.[1,2]

Before leaving this section, it should be noted that all values of the parameters chosen above satisfy the constraint imposed by the similarity form of the linear momentum conservation expressed by equation 13. For all three data sets, $A^2B_u^2 = 0.405 \pm 1\%$. This together with the collapse of the profiles in similarity variables is a necessary consequence of momentum conservation.

D. The turbulence quantities

Figure 7 shows plots of the two components of turbulence intensity available from this experiment, u and w. All show excellent collapse using only U_c and $\delta_{1/2}$ beyond $x/D = 20$. Thus they are consistent with all previous jet measurements;[7,8] and in fact, the swirl seems to have had no effect at all on the second moments. This is consistent with the theoretical prediction of Ewing[3] and confirms the equilibrium similarity approach, at least for the second moments.

Figure 8 plots the correlation coefficient between the two fluctuating velocity components; i.e., $\langle uw \rangle / u_{rms} w_{rms}$. This correlation coefficient is zero to within the statistical and measurement error. This is consistent with in the expected azimuthal homogeneity of the flow, and confirms that the passive role of the mean equation

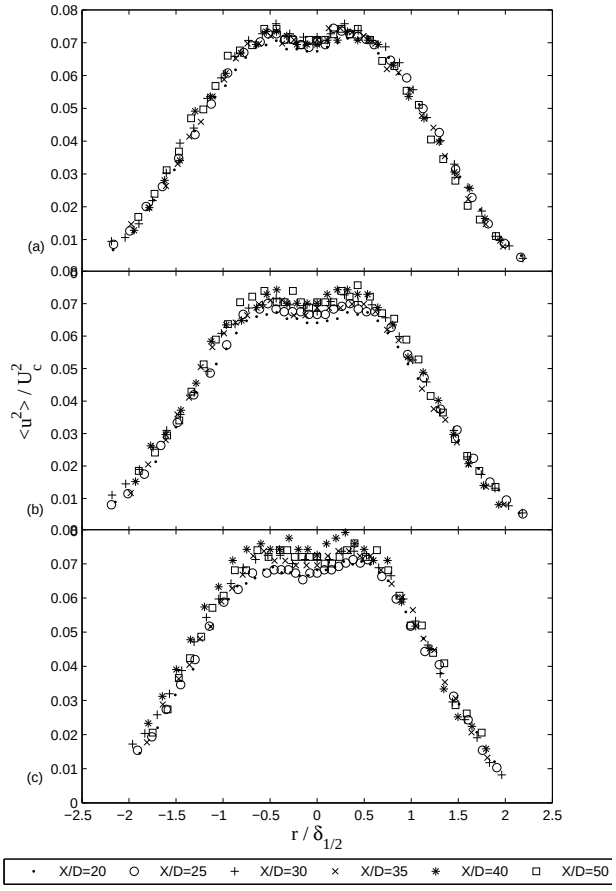

(a) Normalized axial normal stress.

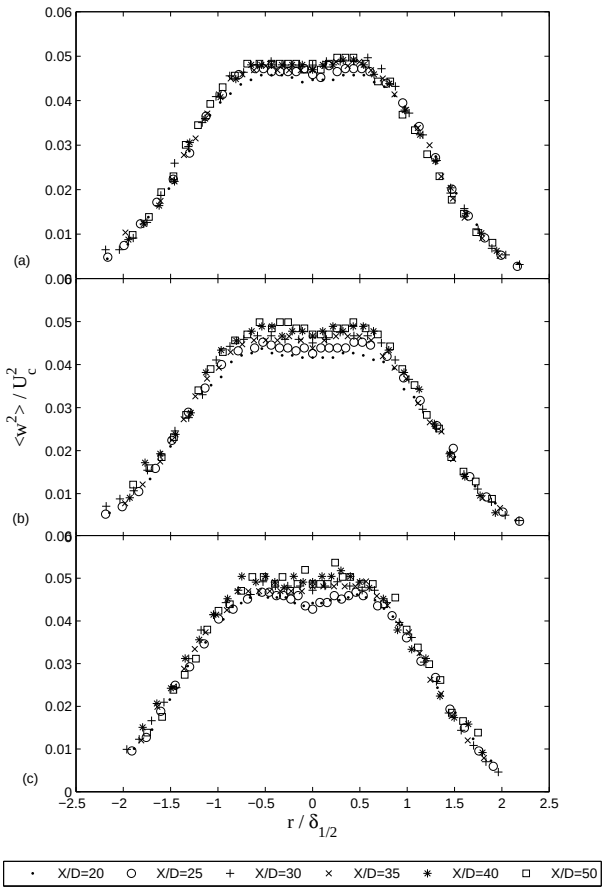

(b) Normalized tangential normal stress.

Figure 7. Normalized plots of u'/U_c and w'/U_c for all positions for different cases (a)S=0, (b)S=0.15, (c)S=0.25.

for W.

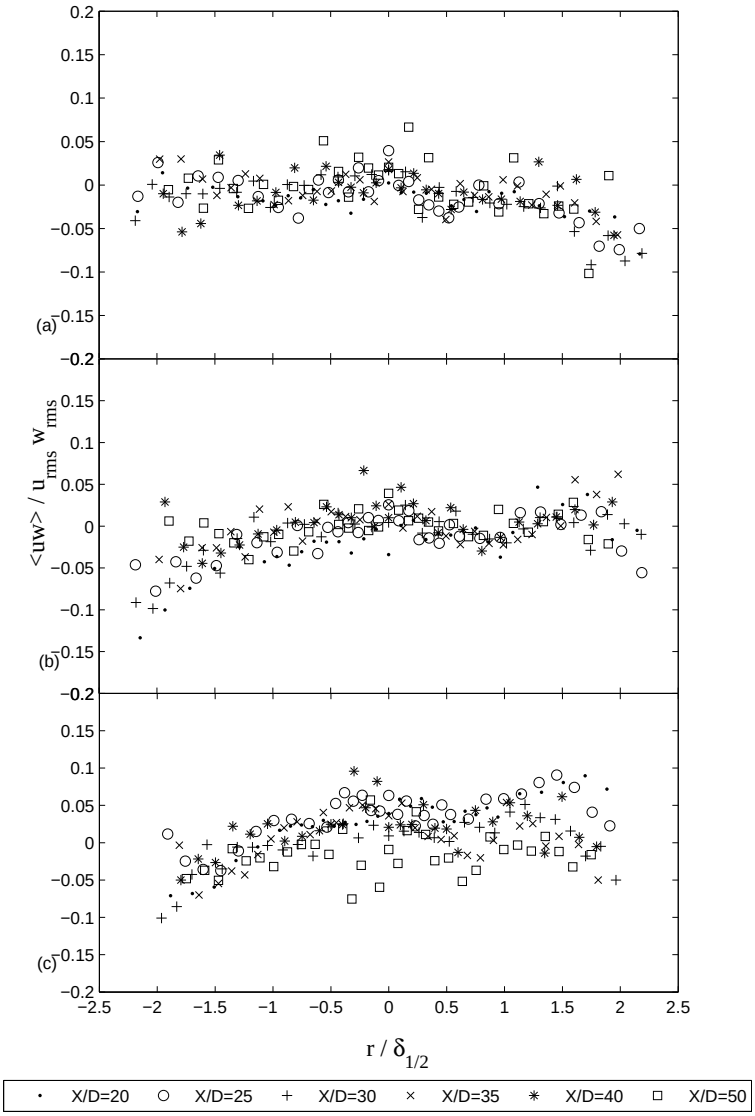

Figure 8. Normalized plots of $\langle uw \rangle / u'w'$ for all positions for different cases (a)S=0, (b)S=0.15, (c)S=0.25.

V. The Vanishing Swirl Velocity

As noted earlier, the measurement of W, the mean swirl component of velocity was the most difficult part of the experiment. Because it is almost two orders of magnitude less than the stream-wise mean velocity at locations of interest, even fractions of a degree difference in the alignment of the laser beams introduces significant errors. Also because of the very low value of W compared to $\langle w^2 \rangle$, there is considerable scatter to the results purely because of the statistical error. Nonetheless, by trying to account for the small offset near the origin and fairing curves through points near the local maxima, it was possible to make an estimate of W_{max} for each of the two values of S.

From conservation of angular momentum and equilibrium similarity it was argued that W_{max} is described by equation 18, and falls off with increasing x as $1/(x - x_o)^2$. Since U_c (described by equation 14) falls as

only $1/(x - x_o)$, then $U_c/W_{max} \propto (x - x_o)$. If it is argued that all of the integrals in similarity variables have constant values (since the normalized profiles are independent of x), the values of C (and B) should be independent of swirl. It follow immediately that slope of U_c/W_{max} should be proportional to M_o/G_o; i.e.,

$$\begin{aligned} \frac{U_c}{W_{max}} &= \frac{C}{B}\,\frac{M_o}{G_o}\,(x - x_o) \\ &= \frac{C}{B}\,S_*^{-1}\,\left[\frac{(x - x_o)}{D_*}\right] \end{aligned} \tag{22}$$

Thus the higher the swirl number, the farther downstream for the swiwl to die off relative to the jet centerline velocity. Alternatively, from the definition of L_* in equation 8 it follows immediately that:

$$\frac{U_c}{W_{max}} = \frac{B}{C}\,\frac{(x - x_o)}{L_*} \tag{23}$$

Thus the role of L_* as a second length scale is clear: it measures the distance for the swirl mean velocity to die off.

Figure 9 plots U_c/W_{max} versus x/D_*. The fitted lines in the figure use the same virtual origins obtained above for the $S = 0.15$ and 0.25 cases; i.e., $x_o 0.75$ and -2.9 respectively. From the considerations of the preceding paragraph, the ratio of the slopes of the two plots should be equal to the the ratio of the values of G_o/M_o itself, which is 0.59. The individual slopes are 0.395 and 0.593 respectively, the ratio of which is 0.66. Thus in spite of the considerable scatter in the measurement of W and the data presented in Figure 9, the overall inferences from them are at the very least, consistent with Ewing's theory.[3]

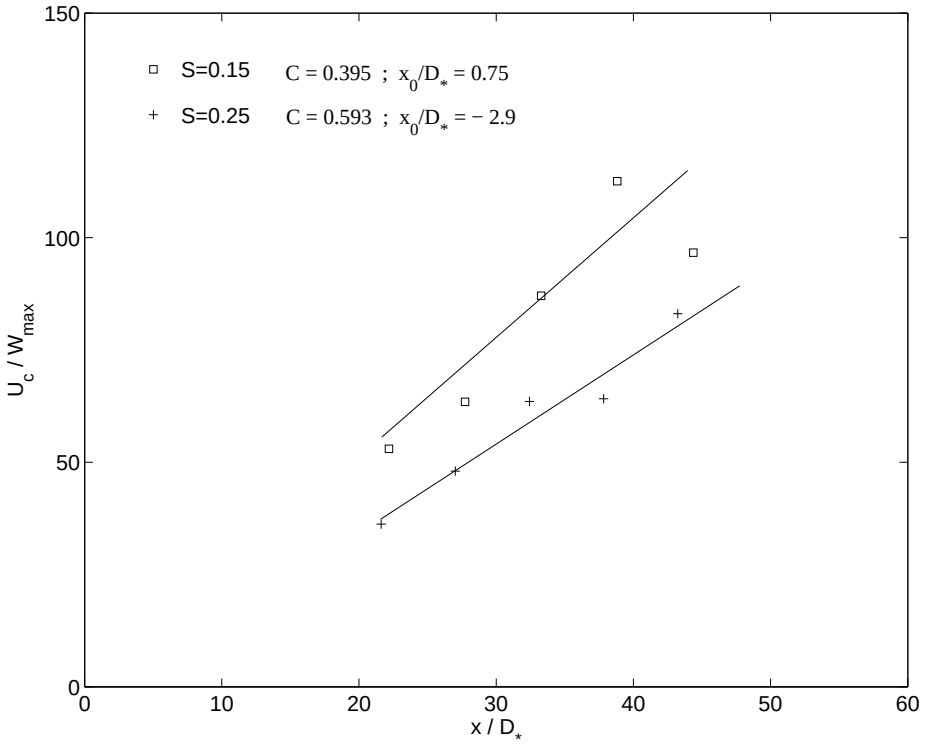

Figure 9. U_c/W_{max} **versus** x/D_* **using the same virtual origins as before; i.e, for** $S = 0.15$, $x_o = 0.75$ **and for** $S0.25$, $x_o = 2.9$

VI. Summary and Conclusions

The far field of an incompressible swirling jet has been studied using two-dimensional laser Doppler anemometry. Three pairs of symmetric injectors were used to produce weak-to-moderate swirling jets. Velocity profiles of the mean and fluctuating stream-wise and azimuthal velocity components were measured in jets with two levels of swirl ($S = 0.15$ and 0.25) at axial locations up to 50 jet exit diameters. The velocity and turbulence intensity profiles, centerline decay, and growth rates for the various swirling jets sere compared to those obtained in the same facility without swirl ($S = 0$). The mean velocity and turbulence intensities collapsed to the same profiles when scaled with the jet centerline velocity and half-width. Thus, like some of the previous observations for the near jet,[1,2] there was no observable effect on the properly scaled far jet for the $S = 0.15$ case. The results were virtually identical to the non-swirling jet. For the $S = 0.25$ case, the only statistically significant effect was a shift in the virtual origin (from $x/D_* = 0.75$ to -2.9).

The recent predictions of equilibrium similarity theory[3] were found to be in excellent agreement with the experimental results. In particular, the mean azimuthal component of velocity falls off as the inverse square of the downstream distance. By contrast, the mean stream-wise velocity and turbulence intensities fall off with simply the inverse of the downstream distance. As a consequence the mean azimuthal equation uncouples from the rest, so the asymptotic swirling jet behaves like the non-swirling jet. A second length scale, L_*, defined from the rates at which momentum and angular momentum are added at the source characterizes the distance which is required for the swirl to become negligible.

Acknowledgements

These measurements were initiated at Chalmers while J. Naugthon was a visiting professor at the Turbulence Research Laboratory. The authors are especially grateful to Dr. T. Gunnar Johansson for his helpful advice and counsel. Dr. D. Ewing also provided useful insight and comments.

References

[1]Chigier, N. and Chervinsky, A., "Experimental Investigation of Swriling Vortex Motion in Jets." *Transaction of the ASME,Journal of Applied Mechanics*, pp. 443–451.

[2]Gilchrist, R. and Naughton, J., "Experimental Study of Incompressible Jets with different Inital Swril Distributions: Mean Results." *AIAA Journal*, Vol. 43, No. 4, 2005, pp. 741–751.

[3]Ewing, D., "Decay of Round Turbulent Jets with Swirl," *Proceedings of the 4th International Symposium on Engineering Turbulence Modeling and Experiments*, Elsvier, 1999.

[4]George, W., "The self-preservation of turbulent flows and its relation to initial conditions and coherent structures," *Advances in Turbulence*, edited by W. George and R. Arndt, Springer, New York, 1989, pp. 39–73.

[5]Mi, J., Nobes, D., and Nathan, G., "Influence of Jet Exit Condition on the Passive Scalar Field of an Axisymmetric Free Jet." *Journal of Fluid Mechanics*, Vol. 432, 2001, pp. 91–125.

[6]Cater, J. and Soria, J., "The evolution of round zero-net-mass-flux jets," *Journal of Fluid Mechanics*, Vol. 472, 2002, pp. 167 – 200.

[7]Panchapakesan, N. and Lumley, J., "Turbulence measurements in Axisymmetric Jets of Air and Helium. Part 1. Air Jet." *Journal of Fluid Mechanics*, Vol. 246, 1993, pp. 197–223.

[8]Hussein, H., Capp, S., and George, W., "Velocity measurements in a high-Reynolds-number, momentum-conserving, axisymmetric, turbulent jet," *Journal of Fluid Mechanics*, Vol. 258, 1994, pp. 31–75.

[9]Farokhi, S., Taghavi, R., and Rice, E., "Effect of Initial Swirl Distribution on the Evolution of a Turbulent Jet." *AIAA Journal*, Vol. 27, No. 6, 1989, pp. 700–706.

[10]Shiri, A., 2006.

[11]Buchhave, P., George, W. K., and Lumley, J. L., "The Measurement of Turbulence with the Laser-Doppler Anemometer," *Annual Review of Fluid Mechanics*, edited by V. Dyke, Wehausen, and Lumley, Vol. 11, Academic Press, Palo Alto, CA., 1979, pp. 443–503.

[12]George, W. K., "Burst-mode Processing of Laser Doppler Anemometer Signals," *Journal of Exp. Thermal and Fluid Science*, Vol. 1, 1988, pp. 48–68.

[13]George, W. K., Beuther, P. D., and Lumley, J. L., "Processing of random signals," *Proceedings of the Dynamic Flow Conference, Lygnby, Denmark*, Dantec, Denmark, 1978, pp. 757–800.

[14]Panda, J. and McLaughlin, D., "Experiments on the Instabilities of a Swirling Jet." *Physics of Fluids*, Vol. 6, No. 1, 1994, pp. 263–276.